Waveform Matching Based Real-time Ablation Monitoring for Microwave Breast Cancer Ablation

Kazuki Kanazawa and Shouhei Kidera,
Graduate school of Informatics and Engineering, The University of Electro-Communications, Japan,
kanazawa.kazuki@ems.cei.uec.ac.jp, kidera@uec.ac.jp

***Abstract*—As a minimal invasive tool for cancer treatment, microwave ablation (MWA) is promising. For safety and effective ablation for cancerous tissue, the real-time monitoring for the dimensions of the ablation zone should be implemented. This study focuses on microwave based MWA monitoring. The time difference of arrival (TDOA) based imaging algorithm is one of most promising methods, which achieves real-time, and highly noise-robust imaging using a prior knowledge of only dielectric constants of tissues surrounding probe, pre and during ablation states. However, it often suffers from an inaccuracy for imaging, especially in the lower impact of the ablation. To enhance the accuracy, this paper proposes the waveform matching based algorithm, where the impact of conductivity drop is also considered in boundary estimation. The statistical test with 100 different ablation cases, using the finite difference time domain (FDTD) simulation, using realistic breast phantoms derived from MRI, demonstrate that the proposed method offers more accurate ablation zone imaging, compared with that obtained by the TDOA based method, maintaining a real-time property.**

***Index Terms*—Microwave ablation(MWA), Microwave based monitoring, Time difference of arrival (TDOA), Waveform matching.**

I. Introduction

Microwave ablation (MWA) technique is widely recognized as a minimal invasive cancer treatment [1], which heats up the cells, more quickly than the lower radio frequency (RF) based technique [2]. The number of literature demonstrated that the MWA becomes an effective clinical tool for treating liver tumors [3]. Such background drives the motivation for applying the MWA to other types of cancer, e.g. kidney or breast tumors. Especially, the MWA treatment for breast tumors brings significant ease for a physical and mental burden for patient by avoiding a large scale removal of breast. For safety and effective ablation for malignant tumors without damaging healthy tissue, the MWA needs to be incorporated with appropriate imaging modality tools. For such imaging modality, magnetic resonance imaging (MRI) and ultrasound based techniques have been developed and tested in the past researches. However, MRI requires a large scale and expensive equipment, and should be need for considering the effect of heating contrast agents [4]. The ultrasound imaging modality is lower and more compact, but there is possibility that microbubbles caused by ablation would contaminate a contrast image [5], as well as limited echogenic contrast between ablated and non-ablated tissue [6]. The microwave based monitoring is promising alternative to address with the above issues, in terms of cost, compactness and compatibility with MWA equipment. It has been demonstrated that the dielectric properties of tissue at microwave frequency are sensitive to the temperature and physiological state of the tissue [7]. Similarly, a recent study also demonstrated that there was a large drop of complex permittivity for tissue in ablated state [8]. The above physical basis drives the development for microwave based ablation monitoring tool, where a forward scattering component received at external antenna from interstitial MWA source is processed by appropriate imaging algorithm. There are several approaches for this kind of algorithms, based on tomographic approach, assuming the fairly homogeneous media, which is a reasonable assumption in liver tissue [9]. However, the method [9] hardly achieves a real-time monitoring, and is not suitable for heterogeneous background, e.g. breast media. As one of the most promising method for real-time and accurate imaging for highly heterogeneous media, the literature [10], the time difference of arrival (TDOA) based imaging algorithm has been developed, which exploits the TDOA of forward scattering signals between before and at a specific time during the ablation. This method has demonstrated, through 2-D and 3-D FDTD based tests, that it simultaneously accomplished a real-time, noise-robust and accurate imaging for ablation zone, even in highly heterogeneous breast tissue. However, there is possibility that it suffers from non-negligible inaccuracy in boundary extraction, especially in the case of a lower impact of dielectric constant in ablated tissue.

To address with the above problem, this paper proposes a waveform reconstruction based imaging method, where a forward scattering signal during ablation is reconstructed from pre-ablation one, using the Green ' s function considering the drops in both real and imaginary parts of complex permittivity as the ablation impact. This method succeeds the significant advantage in the TDOA-based method, that it only requires an estimate of the average relative permittivity and conductivity of the tissue in the vicinity of the MWA antenna at pre- and during ablation, which can be retrieved from temperature monitoring with growing database. The statistical analysis, investigating 100 different ablation cases, using the frequency dependent finite difference time domain (FDTD) and realistic breast phantom, demonstrate that our proposed method offers more accurate estimation of the ablation zone, especially in the case of a lower contrast between pre- and during ablated tissues.

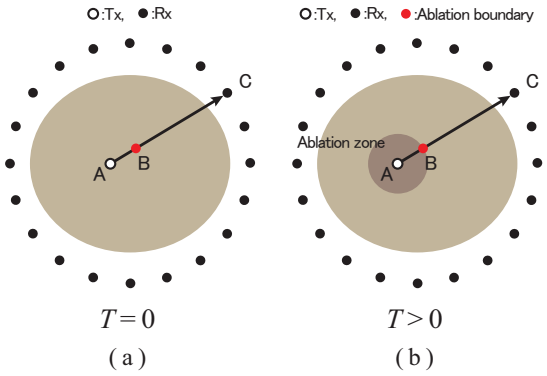

Fig. 1. Data acquisition configuration for MWA monitoring using the internal ablation antenna as the transmitter and an external array as the receivers. (a) Pre-ablation ($T = 0$). (b) During ablation ($T > 0$)

II. Observation Model

Figure 1 shows the data acquisition configuration for our MWA monitoring strategy. The elapsed time of the ablation is denoted by T , where $T = 0$ corresponds to a time pre-ablation and $T > 0$ corresponds to a time during the ablation. A single transmitter (shown as a hollow black circle in Fig. 1) is inserted into the tumor, which is located within the fibrograndular tissue, and multiple receivers are located surrounding the breast (shown as solid black circles in Fig. 1). The location of the source is defined as $\boldsymbol{r}_{\mathrm{A}}$, and the location of a representative receiver is defined as $\boldsymbol{r}_{\mathrm{C}}$. The received microwave signals pre-ablation (at $T = 0$) and during ablation (at the n-th temporal snapshot) are denoted by $s_0(\boldsymbol{r}_{\mathrm{C}}, t)$ and $s_n(\boldsymbol{r}_{\mathrm{C}}, t)$ respectively. The variable t denotes the signal recording time.

III. Ablation Boundary Estimation Algorithm

A. TDOA based method

This method is based on the investigated fact that MWA leads to a decrease of the relative permittivity of tissues, mainly due to dehydration. The lower relative permittivity of the ablation zone leads to a smaller time-delay from source to receiver, compared to the pre-ablation case.

Let τ_0 and τ_n be the times of arrival of the pre- and during ablation signals, received at a location C, respectively. Each time of arrival can be decomposed as follows:

$$\tau_0 = \tau_0^{\mathrm{AB}} + \tau_0^{\mathrm{BC}} \tag{1}$$

$$\tau_n = \tau_n^{\mathrm{AB}} + \tau_n^{\mathrm{BC}}, \tag{2}$$

where τ^{AB} and τ^{BC} denote the time of arrivals from $\boldsymbol{r}_{\mathrm{A}}$ (source location) to $\boldsymbol{r}_{\mathrm{B}}$ (ablation boundary point), and $\boldsymbol{r}_{\mathrm{B}}$ to $\boldsymbol{r}_{\mathrm{C}}$ (receiver location), respectively, as shown in Fig. 1. We define ϵ_n^{AB} as the dielectric constant of the tissue inside the ablation zone at the n-th snapshot, and ϵ_0^{AB} represents the dielectric constant pre-ablation. In addition, $\tau_0^{\mathrm{BC}} \simeq \tau_n^{\mathrm{BC}}$, because the dielectric properties of the tissue between B and C are invariant. Then, the TDOA between pre- and during ablation cases can be expressed approximately as follows:

$$\begin{aligned} \Delta\tau &\equiv \tau_0 - \tau_n \\ &\simeq (1 - \sqrt{\xi})\tau_0^{\mathrm{AB}}, \end{aligned} \tag{3}$$

where $\xi = \epsilon_n^{\mathrm{AB}}/\epsilon_0^{\mathrm{AB}}$. From Eq. (3), we can estimate the distance from source to boundary point as follows:

$$\begin{aligned} R^{\mathrm{AB}} \equiv ||\boldsymbol{r}_{\mathrm{A}} - \boldsymbol{r}_{\mathrm{B}}|| &\simeq v_0 \tau_0^{\mathrm{AB}} \\ &\simeq v_0 \frac{\Delta\tau}{1 - \sqrt{\xi}}, \end{aligned} \tag{4}$$

where v_0 denotes the propagation velocity in the pre-ablation medium. Then, the ablation boundary point $\boldsymbol{r}_{\mathrm{B}}$ is given by:

$$\boldsymbol{r}_{\mathrm{B}} = R^{\mathrm{AB}}\boldsymbol{u} + \boldsymbol{r}_{\mathrm{A}}, \tag{5}$$

where $\boldsymbol{u}$ denotes a unit vector from $\boldsymbol{r}_{\mathrm{A}}$ to $\boldsymbol{r}_{\mathrm{C}}$.

Note that, $\Delta\tau$ can be estimated from the following cross-correlation calculation:

$$\Delta\tau = \arg\max_{\tau} \left[s_0(\boldsymbol{r}_{\mathrm{C}}, t) \star s_n(\boldsymbol{r}_{\mathrm{C}}, t) \right](\tau), \tag{6}$$

where $\star$ denotes the operator of cross-correlation. If the number of receivers is M, then M different boundary points $\boldsymbol{r}_{\mathrm{B}}$ can be estimated.

The most notable feature of this method is that it only requires the following as a priori knowledge: 1) an estimate of the average velocity in the medium surrounding the source before the ablation begins, and 2) an estimate of the ratio of the pre-ablation and ablated-tissue dielectric constant in the target region.

B. Proposed method

While a number of tests have demonstrated that the above TDOA-based method is fast enough for real-time ablation monitoring and is robust against noise, this algorithm does not consider the impact of the decrease in conductivity that tissue experiences as it dries out. This decrease in conductivity affects not only the amplitude of the forward-scattered signal, but it also affects the phase of the signal. Waveform reconstruction to recover this phase information could further improve the accuracy for ablation imaging.

Assuming the simple propagation model used in the TDOA based method, the proposed method also models the pre- and during ablation signal in the angular frequency domain, under the straight line propagation assumption, as:

$$S_0(\omega; R^{\mathrm{AB}}) = S_{\mathrm{src}}(\omega) e^{-j(k_0(\omega)R^{\mathrm{AB}} + k(\omega)R^{\mathrm{BC}})} \tag{7}$$

$$S_n(\omega; R^{\mathrm{AB}}) = S_{\mathrm{src}}(\omega) e^{-j(k_n(\omega)R^{\mathrm{AB}} + k(\omega)R^{\mathrm{BC}})}, \tag{8}$$

where $S_0(\omega; R^{\mathrm{AB}})$ and $S_n(\omega; R^{\mathrm{AB}})$ denote the received signals at pre- and during ablation state at n-th snapshot in the angular frequency domain. Here, the wavenumber at the n-th snapshot as $k_n(\omega)$ is expressed as:

$$k_n(\omega) = \beta_n(\omega) - j\alpha_n(\omega), \tag{9}$$

where $\alpha_n(\omega)$ and $\beta_n(\omega)$ are defined as:

$$\alpha_n(\omega) = \omega\sqrt{\mu\epsilon_n}\left[\frac{1}{2}\sqrt{1+\frac{\sigma_n^2}{\omega^2\epsilon_n^2}}-\frac{1}{2}\right]^{\frac{1}{2}} \tag{10}$$

$$\beta_n(\omega) = -\omega\sqrt{\mu\epsilon_n}\left[\frac{1}{2}\sqrt{1+\frac{\sigma_n^2}{\omega^2\epsilon_n^2}}+\frac{1}{2}\right]^{\frac{1}{2}}. \tag{11}$$

Here, ϵ_n and σ_n are the relative permittivity and conductivity in the ablation state at the n-th snapshot, where R^{BC} denote the distance from $\boldsymbol{r}_{\mathrm{B}}$ to $\boldsymbol{r}_{\mathrm{C}}$ (receiver location). Using this model, the signal at the n-th snapshot ablation state is estimated as:

$$\hat{S}_n(\omega; R^{\mathrm{AB}}) = S_0(\omega; R^{\mathrm{AB}}) \cdot e^{-j(k_n(\omega)-k_0(\omega))R^{\mathrm{AB}}}. \tag{12}$$

Finally, the distance from the source to the ablation boundary at the n-th snapshot as R_n^{AB} calculated as:

$$\hat{R}_n^{\mathrm{AB}} = \arg\min_{R^{\mathrm{AB}}} \int |\hat{S}_n(\omega; R^{\mathrm{AB}}) - S_n^{\mathrm{obs}}(\omega)|^2 d\omega, \tag{13}$$

where $S_n^{\mathrm{obs}}(\omega)$ denotes the observation signal in the angular frequency domain at the n-th snapshot.

The procedure for the proposed method is summarized as follows:

Step 1) Received signals are recorded at $T = 0$ (before the ablation begins) and at the n-th temporal snapshot during the ablation.

Step 2) Noise reduction filter (e.g. matched filter), is applied to both observed signals.

Step 3) Waveform in the n-th snapshot in the ablation state is derived in Eq. (12).

Step 4) $\hat{R}_n^{\mathrm{AB}}$ is determined in Eq. (13) and ablation boundary point $\boldsymbol{r}_{\mathrm{B}}$ is determined in Eq. (5).

This method maintains most of advantages in the conventional TDOA-based method that it only requires the ratio of the pre-ablation and during ablation dielectric constant and conductivity in the target region as a priori knowledge. In most cases, the source will be located inside malignant tissue, whose dielectric properties are available in the literature [11].

IV. Two-Dimensional Numerical Simulation Examples

A. Brest phantom and simulated array measurements

We tested our method using simulated measurements of two realistic breast phantoms derived from MRIs of healthy women [11]: a Class 3 "heterogeneously dense" phantom (ID number 062204), and a Class 4 "very dense" (ID number 012304) phantom. These phantoms are available online at the University of Wisconsin repository [12]. The frequency dependent complex permittivities for skin and breast tissues in the phantoms are modeled by single-pole Debye models over the frequency range from 0.1 to 5.0 GHz, as in [9]. Figure. 2 shows the map of the Debye parameter $\Delta\epsilon$ of the Class 3 and Class 4 phantoms. The transmitting source, shown as a hollow black circle in Fig. 2, is located inside fibroglandular tissue. The average pre-ablation relative permittivity and conductivity of the tissue surrounding the antenna was $\epsilon_0^{\mathrm{AB}} = 42, \sigma_0^{\mathrm{AB}}$ =0.633 S/m, which corresponds to the median value for healthy fibroglandular tissue at $f_0 = 2.45$ GHz. The 20 receiving antennas, shown as solid black circles in Fig. 2, are located on a ring outside breast (immersed in air) with equal spacing between them. Here, we conducted 2-D FDTD simulations with single-pole Debye model (in-house code provided by the cross-disciplinary electromagnetics laboratory at the University of Wisconsin, Madison).

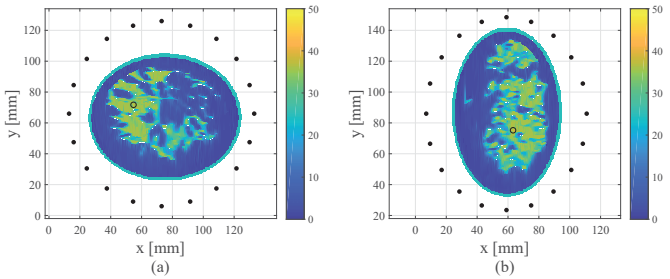

Fig. 2. 2-D numerical breast phantom and configuration used to evaluate the performance of the MWA monitoring algorithm using Amplitude and Phase information. The colorbar displays the Debye parameter, $\Delta\varepsilon$. The hollow black circle denotes the location of the transmitting antenna while the solid circles denote the locations of the receiving antennas. (a) Class 3 (heterogeneously dense) breast phantom. (b) Class 4 (extremely dense) breast phantom.

The transmitted signal is a Gaussian modulated pulse, with 2.45 GHz as the center frequency and a 1.9 GHz full 3 dB bandwidth. The received signals are computed using FDTD on a 0.5 mm grid. White Gaussian noise is added to each recorded electric field temporal waveform. The SNR is defined as the ratio of the average signal power to noise power in the time domain. We consider SNR levels of 20 dB. These are assumed to uniformly decrease in the ablation zone, therefore the dielectric properties in the ablation zone are also heterogeneous. We have modeled the $\xi = 0.6$, 0.7, 0.8, and 0.9 in both relative permittivity and conductivity, as the influence of ablation. This percentage range has been observed in ablations of bovine liver tissue [7] and human mastectomy specimens [8].

B. Imaging results and discussions

Here, we test the particular snapshot during the ablation, where the ablation zone is expressed as an ellipse spanning 20 mm along the x-axis and 16 mm along the y-axis. Figures 3 shows the estimated ablation zone by each method, at the Class 3 and Class 4 phantoms, where $\xi = 0.9$ and noiseless situation is assumed. Figure 3 validates that the proposed method significantly enhances the accuracy for boundary extraction in the ablation zone. Here, the normalized root mean square error (NRMSE) is introduced to investigate the accuracy for

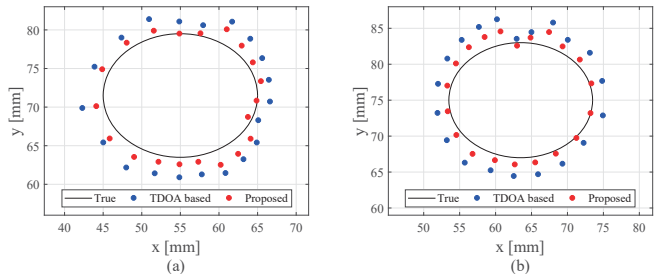

Fig. 3. Estimated boundaries of the elliptical ablation zone in noiseless case. Blue solid circles by the TDOA-based method, and red solid circles by the proposed method. The actual ablation zone is an ellipse with major radius (x-axis) of 10 mm and minor radius (y-axis) of 8 mm. (a): Class 3. (b): Class4.

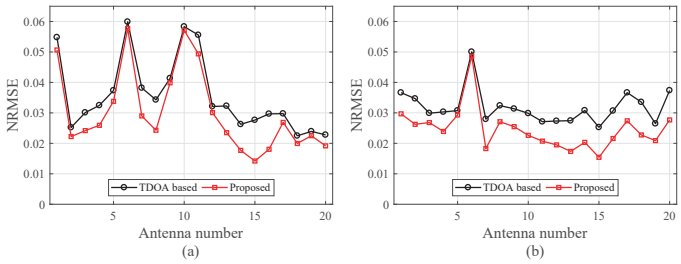

Fig. 4. NRMSE for waveform reconstruction at different antenna location. Black line denotes the result of the TDOA based method, and red one denotes that of the proposed method. (a): Class 3. (b): Class 4.

the waveform reconstruction for the observed waveforms as:

$$\mathrm{NRMSE}_n = \sqrt{\frac{\int_0^T |\hat{s}_n(t) - s_n^{\mathrm{obs}}(t)|^2 dt}{\int_0^T |s_n^{\mathrm{obs}}(t)|^2 dt}}, \qquad (14)$$

where $\hat{s}_n(t)$ denotes the estimated scattering signal by each method. Note that, the time-shift of $\hat{s}_n(t)$ of the TDOA-based method is compensated using the time-delay $\Delta\tau$ calculated in Eq. (6). Figure 4 shows the NRMSE for each antenna location in Class 3 and Class 4 phantoms. This results indicates that the proposed method achieves more accurate waveform reconstruction compared with that obtained by the TDOA-based method by considering the influence of conductivity drop. Better waveform matching enhances the accuracy for estimation of R_n^{AB}, results in better imaging. Note that, the average calculation times are 0.1 sec in the TDOA-based method and 0.3 sec in the proposed method using an Intel Xeon CPU E5-1620 v2 3.7 GHz, with 16 GB RAM.

C. Statistical tests for various centers of ablation zone

This section describes the statistical tests in each method. The 100 different patterns of the ablation center are investigated in both Class 3 and Class 4 phantoms, where the dimension of the ablation is fixed and same in the Sec. IV-B. Here, we define the reconstruction error for a specific estimated boundary point, $\boldsymbol{r}_{\mathrm{B}}$, as the shortest distance from that estimated boundary point to the actual boundary. Figure 5 show the box plots of the median value of the estimation errors in Class 3 phantom for the TDOA based and the proposed methods at each value of ablation factor (ξ) for the cases of noiseless and 20 dB SNR. Figure 6 show the box plots of the estimation errors in Class 4 using same configuration in Fig. 5. The lower and upper bounds of the boxes span the IQR (interquartile range) and the lower and upper whisks denote the ± 2.7 standard deviation range. These results demonstrate that the proposed method enhances the accuracy in any case of ξ and SNRs. The difference is remarkable, particularly in case the ablation factor ξ =0.9, where the TDOA-based method suffers from significant inaccuracy. This is because the small decrease of dielectric constant leads to smaller time-shift $\Delta\tau$, and the sensitivity to the error of $\Delta\tau$ becomes more severe in the method based on only the TDOA values. On the contrary, the proposed method can enhance the accuracy of $\Delta\tau$ by compensating the waveform deformation with conductivity drop.

V. Conclusion

This paper proposed the waveform matching based estimation method for the dimension of the ablation zone, where the impact of dielectric property drop is considered in not only the relative permittivity but the conductivity. The proposed algorithm compensated the waveform mismatching between pre- and during ablation signals, which enhances the accuracy in R^{AB} estimation, especially in the higher ξ case. The numerical investigations with 100 different samples, demonstrate that the proposed algorithm significantly achieves more accurate boundary extraction for MWA monitoring even in situations of high ablation factor as ξ. This method requires further investigations in the three-dimension model and the experimental data.

Acknowledgment

This research and development work was supported by the MIC/SCOPE #162103102.

References

[1] Arye Rosen, Maria A. Stuchly, and Andr Vander Vorst, "Applications of RF/Microwaves in Medicine" *IEEE Transactions on Microwave Theory and Techniques*, Vol. 50, Mar. 2002.

[2] G. Carrafiello, D. Lagana, M. Mangini, F. Fontana, G. Dionigi, L. Boni, F. Rovera, S. Cuffari and C. Fugazzola, "Microwave tumors ablation: Principles, clinical applications and review of preliminary experiences" *Int. J. Surg.* S65-9, Dec. 2008.

[3] R. C. G. Martin, C. R. Scoggins and K. M. McMasters, "Safety and efficacy of microwave ablation of hepatic tumours: a prospective review of a 5-year experience" *Ann. Surg. Oncol.* 17 171-8, Jan. 2010

[4] L. G. Merckel, L. W. Bartels, M. O. Kohler, H. J. G. D. van den Bongard, R. Deckers, W. Mali, C. Binkert, C. T. Moonen, K G. A. Gilhuijs, and M. A. A. J. van den Bosch" MR-guided high-intensity focused ultrasound ablation of breast cancer with a dedicated breast platform, "*Cardiovasc. Intervent. Radiol.*, vol. 36, no. 2, pp. 292 301. Apr. 2013.

[5] Correa-Gallego, M. D., A. M. Karkar, S. Monette, P. C. Ezell, W. R. Jarnagin, and T. P. Kingham, "Intraoperative ultrasound and tissue elastography measurements do not predict the size of hepatic microwave ablations," *Acad. Radiol.*, vol. 21, no. 1. pp. 7278, Jan. 2014.

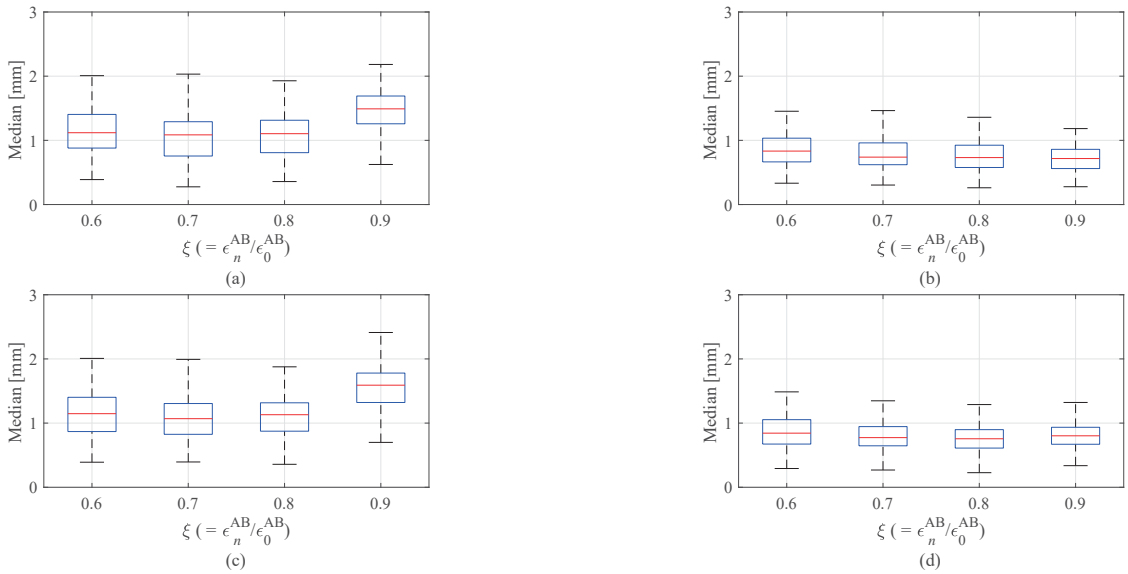

Fig. 5. Median errors in ablation zone boundary estimation as a function of ξ for 100 different centers of ablation zone in Class 3 phantom. (a) TDOA-based method at SNR= ∞. (b) Proposed method at SNR= ∞. (c) TDOA-based method at SNR=20 dB. (d) Proposed method at SNR=20 dB.

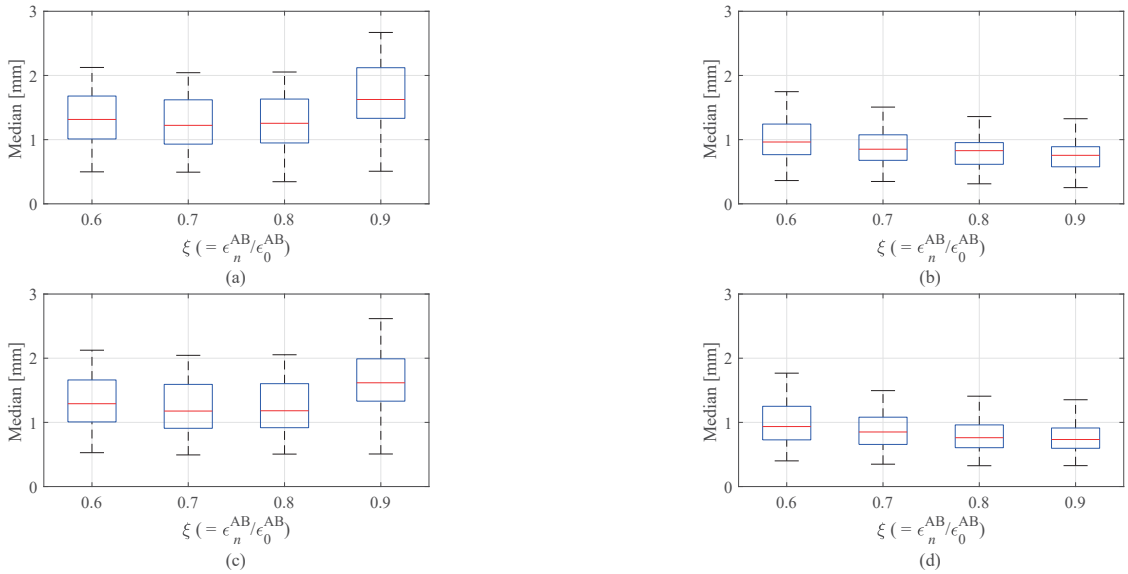

Fig. 6. Median errors in ablation zone boundary estimation as a function of ξ for 100 different centers of ablation zone in Class 4 phantom. (a) TDOA-based method at SNR= ∞. (b) Proposed method at SNR= ∞. (c) TDOA-based method at SNR=20 dB. (d) Proposed method at SNR=20 dB.

[6] W. Yang, M. Alexander, N. Rubert, A. Ingle, M. Lubner, T. Ziemlewicz, J. L. Hinshaw, F. T. Lee Jr, J. A. Zagzebski, T. Varghese, "Monitoring Microwave Ablation for Liver Tumors with Electrode Displacement Strain Imaging", *Proc. of 2014 IEEE International Ultrasonics Symposium (IUS)*, Sept. 2014.

[7] V. Lopresto, R. Pinto, G. A Lovisolo, and M. Cavagnaro, "Changes in the dielectric properties of ex vivo bovine liver during microwave thermal ablation at 2.45 GHz", *Phys. Med. Biol.* vol. 57, pp. 2309 -2327, 2012.

[8] R. O. Mays, L. M. Neira, A. Schulman, J. Harter, L. G. Wilke, N. Behdad, and S. C. Hagness, "A pilot study of microwave ablation in ex vivo human breast tissue," *Proc. of USNC/URSI National Radio Science Meeting*, Puerto Rico, June 2016.

[9] O. M. Bucci, M. Cavagnaro, L. Crocco, V. Lopresto and R. Scapaticci, "Microwave Ablation Monitoring via Microwave Tomography: a Numerical Feasibility Assessment", *Proc. of 2016 10th European Conference on Antennas and Propagation*, 2016.

[10] Shouhei Kidera, Luz Maria Neira, Barry D. Van Veen, and Susan C. Hagness, "TDOA-Based Microwave Imaging Algorithm for Real-Time Monitoring of Microwave Ablation" *Proc. of 2017 11th European Conference on Antennas and Propagation (EuCAP)*, March, 2017.

[11] M. Lazebnik, D. Popovic, L. McCartney, C. B.Watkins, M. J. Lindstrom, J. Harter, S. Sewall, T. Ogilvie, A. Magliocco, T. M. Breslin, W. Temple, D. Mew, J. H. Booske, M. Okoniewski, and S. C. Hagness, "A large-scale study of the ultrawideband microwave dielectric properties of normal, benign, and malignant breast tissues obtained from cancer surgeries," *Physics in Medicine and Biology*, vol. 52, pp. 6093-6115, 2007.

[12] University of Wisconsin Cross-Disciplinary Electromagnetics Laboratory (UWCEM), "Numerical breast phantom repository" [Online]. Available: http://uwcem.ece.wisc.edu, accessed on: October 2, 2017.